

Mechanism of Microemulsion Polymerization of Methyl Methacrylate: Experimental Evidence

SANTANU ROY and SUREKHA DEVI*

Department of Chemistry, M.S. University of Baroda, Baroda 390 002, India

SYNOPSIS

Free radical polymerization of methyl methacrylate in emulsion and microemulsion media was studied for the understanding of the mechanism of the polymerization process. Average particle size of the poly(methyl methacrylate) (PMMA) latex formed during microemulsion polymerization was observed to be ~ 45 nm. Nuclear magnetic resonance data indicated a larger number of interactions for β -methylene protons of PMMA synthesized in microemulsion, indicating dominant isotacticity in the polymer. Activation energy of degradation of the products was calculated by Broido's method and was found to be 44.70 kJ/mol and 65.47 kJ/mol for PMMA synthesized from microemulsion and emulsion media, respectively. Solution properties of the above polymers were also studied. Intramolecular expansion factors indicate a more rigid structure for PMMA synthesized from microemulsion medium.

© 1996 John Wiley & Sons, Inc.

INTRODUCTION

Microemulsion polymerization is gaining interest in recent years due to more ordered assemblies, which influence the properties of the polymeric products. The first microemulsion polymerization of methyl methacrylate (MMA) was reported by Stoffer and Bone¹ for w/o systems using water and oil-soluble initiators. They have reported that the increased initiator concentration resulted in products with decreased weight-average molecular weight (\bar{M}_w) and high polydispersity, as observed in the classical emulsion polymerization. Polymerization of MMA and styrene was reported by Jaykrishnan and Shah² and Feng and Ng.³ Slower polymerization rates were observed for microemulsion polymerization than for emulsion polymerization by Jaykrishnan and Shah.² They have also reported loss of transparency and stability of microemulsion during the polymerization process. Feng and Ng³ reported number-average molecular

weight (\bar{M}_n) values of 10^5 range and polydispersity around 4.5 for the products obtained. The initial rate of polymerization of MMA in o/w microemulsion was observed to be faster than that of styrene. Gan and coworkers⁴ studied ternary systems containing water, MMA, and cetyl trimethyl ammonium bromide in which turbid emulsions were changed to transparent microemulsions with increasing surfactant concentration. Stable poly(methyl methacrylate) (PMMA) latexes of 16 to 30 nm hydrodynamic radii and molecular weights in the $5-7 \times 10^6$ range were obtained from emulsion and microemulsion media.

In conventional emulsion polymerization the principle loci for initiation of latex particles are assumed to be the monomer-swollen micelles^{5,6} and aqueous phase.⁷⁻⁹ Monomer droplets act as reservoirs during polymerization. In microemulsion polymerization the monomer droplets stabilized by surfactant are the principle loci for polymerization. This difference in mechanism of polymerization is assumed to influence the stereoregularity and hence thermal properties of the products. In this paper we have attempted to correlate these properties with the polymerization mechanism.

* To whom correspondence should be addressed.

Table I Microemulsion and Emulsion Recipe

	Microemulsion		Emulsion	
	Weight (g)	Percent (w/w)	Weight (g)	Percent (w/w)
Water	46.2	76.1	46.2	87.7
SDS	8.5	14.0	0.5	0.9
MMA	6.0	9.9	6.0	11.4

EXPERIMENTAL

Materials

AR grade MMA from Sisco-chem, Bombay, India, was purified by treating with 5% sodium hydroxide solution followed by washings with deionized water. Further, it was dried over fused calcium chloride and then vacuum-distilled under nitrogen atmosphere. Potassium persulphate (KPS) (Sisco-chem) and sodium dodecyl sulphate (SDS) (Qualigen, Glaxo, Bombay, India) of extra-pure grade were used without further purification. Double-distilled deionized water was used throughout the work.

Synthesis

The recipe used for the emulsion and microemulsion polymerization is given in Table I. The reaction mixture was heated to the optimized temperature (80°C). The requisite amount (1.25 mM) of KPS, dissolved in a minimum quantity of water, was added. The reaction was carried out under nitrogen atmosphere. The rate of polymerization was determined by withdrawing 5 mL of the reaction mixture at different time intervals and arresting the reaction by adding 20 ppm of hydroquinone and then precipitating the polymer with methanol. Percent conversion was calculated gravimetrically.

Characterization

Average particle size of polymerized microemulsion was determined using a JEOL-JEM 100SX transmission electron microscope and uranyl acetate as staining reagent. A drop of polymerized latex was added to 2 mL of 2% uranyl acetate solution. One drop of this diluted latex was put on a copper grid which had been coated with thin layer of formvar. Average particle size was calculated by considering 100 particles per 25 cm².

Volume average size, median diameter, and particle size distribution were determined by using a Brookhaven (USA) B90 Particle Size Analyzer.

Water GPC 150C was used to determine M_n and M_w and polydispersity using tetrahydrofuran solvent.

High-resolution ¹H-NMR of the polymers were recorded in CDCl₃ on a 500 MHz Bruker nuclear magnetic resonance (NMR) spectrophotometer.

Thermogravimetric analysis (TGA) was carried out in pure nitrogen atmosphere, at a 10°C/min heating rate.

Viscosity measurements of the dilute solutions containing 0.3 to 1.0 g/dL of the polymer in acetone were carried out using a Ubbelohde dilution viscometer suspended in a thermostated bath with ±0.05°C temperature control.

RESULTS AND DISCUSSION

The microemulsions under study were transparent isotropic and thermodynamically stable. The polymerized microemulsions were stable but translucent due to the increase in the size of the dispersed phase. The microemulsion recipe was selected from the partial phase diagram of SDS/MMA/water at 27°C (Fig. 1). The clear-turbid boundaries were established from systematic titrations.

Kinetics of Polymerization

Kinetics of MMA polymerization in the emulsion and microemulsion media (Table I recipe) were studied at 80°C temperature and 1.25 mM KPS

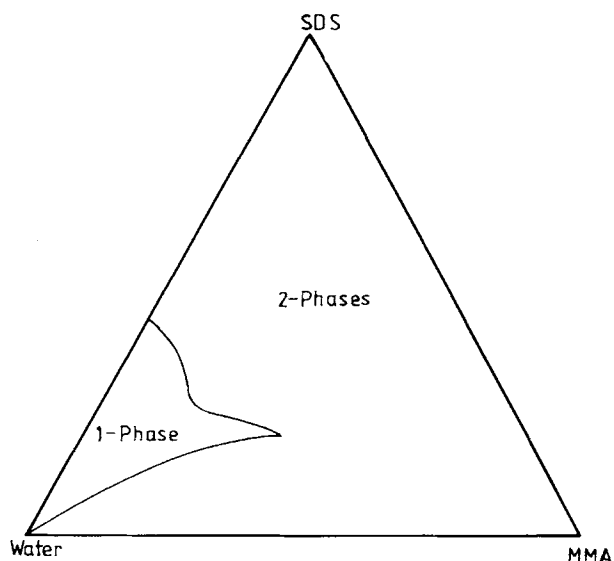


Figure 1 Partial phase diagram of SDS-water-MMA at 27°C.

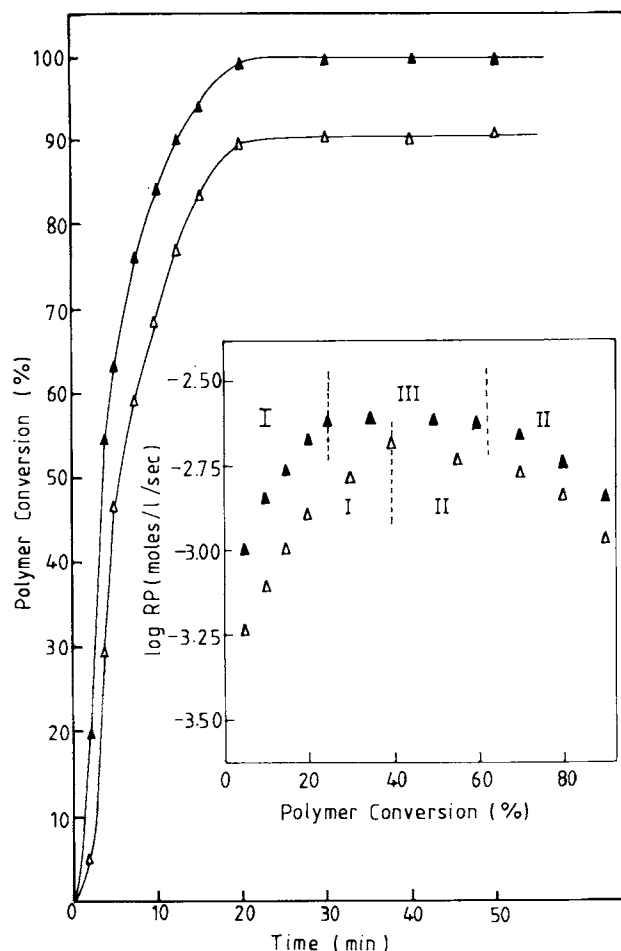


Figure 2 Percent conversion versus time and polymerization rate versus % conversion plots for (Δ) MMA-ME and (\blacktriangle) MMA-E; KPS concentration 1.25 mM, temperature 80°C.

concentration. The results obtained are given as percent conversion versus time plots in Figure 2. It was observed that the rate of polymerization is slower in microemulsion than in emulsion. A similar observation was made by Jaykrishnan and Shah.² Tang and colleagues¹⁰ also reported an extremely long polymerization duration (8 days at 50°C in nitrogen atmosphere) for styrene. However, high rates of polymerization for styrene with a leveling off at 80 to 90% within 60 min was observed by Guo and coworkers¹¹ and others.^{12,13} We have observed in the present study of polymerization of MMA in microemulsion that leveling off takes place at 90% conversion within 20 min (Fig. 2). The maximum polymerization rate in microemulsion is observed at relatively high conversions (40% conversion) as compared with emulsion polymerization (25% conversion). The polymerization rate versus percent

conversion plots show two distinct regions for microemulsion polymerization. Interval I is considered to be the nucleation stage, which is characterized by an increase in the rate of polymerization due to an increase in the number of polymerizing loci with time. In interval II the polymerization rate decreases due to decreased monomer concentration in the monomer-swollen polymer particles. Similar rate intervals were observed for microemulsion polymerization of styrene and MMA by Guo and coworkers¹¹ and Gan and colleagues,⁴ respectively. However, emulsion polymerization exhibits three regions. The additional III region is assigned to the

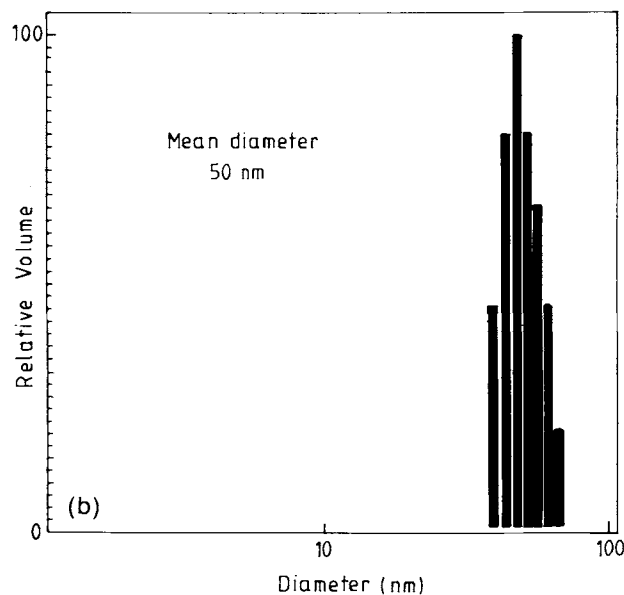
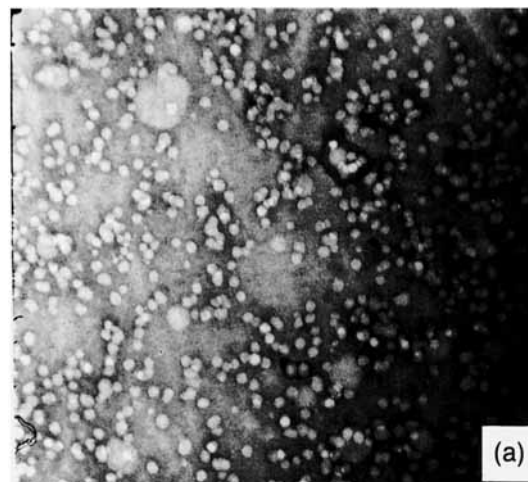


Figure 3 (a) Transmission electron micrograph of latex particles from microemulsion polymerization (Magnification: $\times 25,000$). (b) Particle size distribution in microemulsion latex of PMMA.

Table II High Resolution ¹H-NMR Data for Homopolymers of MMA Synthesized in Microemulsion (PMMA-ME) and Emulsion Media (PMMA-E)

PMMA-ME				PMMA-E			
Peak	Frequency		Intensity	Peak	Frequency		Intensity
	[Hz]	[PPM]			[Hz]	[PPM]	
1.	1796.71	3.5925	20.00	1.	1793.79	3.5866	20.00
2.	1028.75	2.0569	0.25	2.	942.94	1.8854	2.94
3.	1014.63	2.0287	0.29	3.	900.93	1.8014	4.93
4.	969.89	1.9393	0.86	4.	713.84	1.4273	0.86
5.	947.20	1.8939	1.28	5.	599.63	1.1989	0.92
6.	934.04	1.8676	1.04	6.	503.85	1.0074	6.70
7.	902.96	1.8054	3.83	7.	417.18	0.8341	8.78
8.	715.02	1.4297	0.48				
9.	603.10	1.2059	0.56				
10.	506.59	1.0129	4.93				
11.	420.75	0.8413	5.51				
12.	414.43	0.8286	5.45				

steady-state polymerization. During this stage polymerization takes place by diffusion of monomer from monomer droplets, acting as reservoirs. In 1946, Baxendale and coworkers¹⁴ suggested homogeneous nucleation in aqueous phase for emulsion polymerization of MMA. The rate of polymerization was observed to remain constant up to high conversions of MMA. Zimmt¹⁵ also reported a constant rate of polymerization for MMA with swollen particles' diameters less than 100 nm due to steady-state polymerization rate. Due to relatively high solubility of MMA, a considerable amount (0.15 mol/dm³) of it remains dissolved in the aqueous phase. Hence homogeneous nucleation should be important both in emulsion and microemulsion polymerization of MMA. Due to a very small amount of surfactant, the number of monomer swollen micelles is less in emulsion than the number of monomer droplets stabilized by surfactant. Hence the amount of MMA in monomer-swollen micelles as well as in the aqueous phase of emulsion will be significant. However a large amount of MMA will remain in monomer droplets acting as reservoirs; whereas, in the case of microemulsions, mainly monomer droplets stabilized by surfactant are present, which act as monomer-swollen micelles and not as monomer reservoirs. Hence there will be a large difference in the concentration of MMA in surfactant-stabilized monomer droplets and MMA in aqueous phase. As a result the free radicals generated from KPS in the aqueous phase react with MMA through the usual micellar nucleation and also by homogeneous nucleation mechanism in emulsions; whereas in mi-

croemulsion, initiation takes place mainly at the monomer droplets which act as monomer-swollen micelles. We have observed nucleation mainly in monomer droplets in o/w microemulsion polymerization of MMA through NMR, thermal, and viscosity studies of PMMA.

Particle Size and Molecular Weight

Figure 3(a,b) illustrates the transmission electron micrograph (TEM) and particle size distribution plots from light scattering of polymerized microemulsion latexes of MMA. Average particle size was calculated considering at least 100 particles per 25 cm² of TEM micrographs. For microemulsion polymers the average size was ~ 45 nm while for emulsion polymers it was ~ 75 nm. The small size of the emulsion latex was due to the low monomer concentration (11%) of the recipe under study. In emulsion polymerization the initiation of polymerization takes place in the monomer-swollen micelles or at the aqueous phase. The particles then grow by diffusion of monomer from the monomer reservoirs. As the concentration of monomer is less, the particle size achieved is only 75 nm. The particle size measured by means of light scattering technique gave a mean diameter of 50 nm for polymerized microemulsion latex. It was found that 10% of the particles were below 37 nm, 25% below 42 nm, 50% below 47 nm, 75% below 54 nm, and 90% below 61 nm.

PMMA synthesized from microemulsion medium showed \bar{M}_w 8.03×10^5 , \bar{M}_n 1.72×10^5 , and polydispersity 4.66; whereas PMMA synthesized from

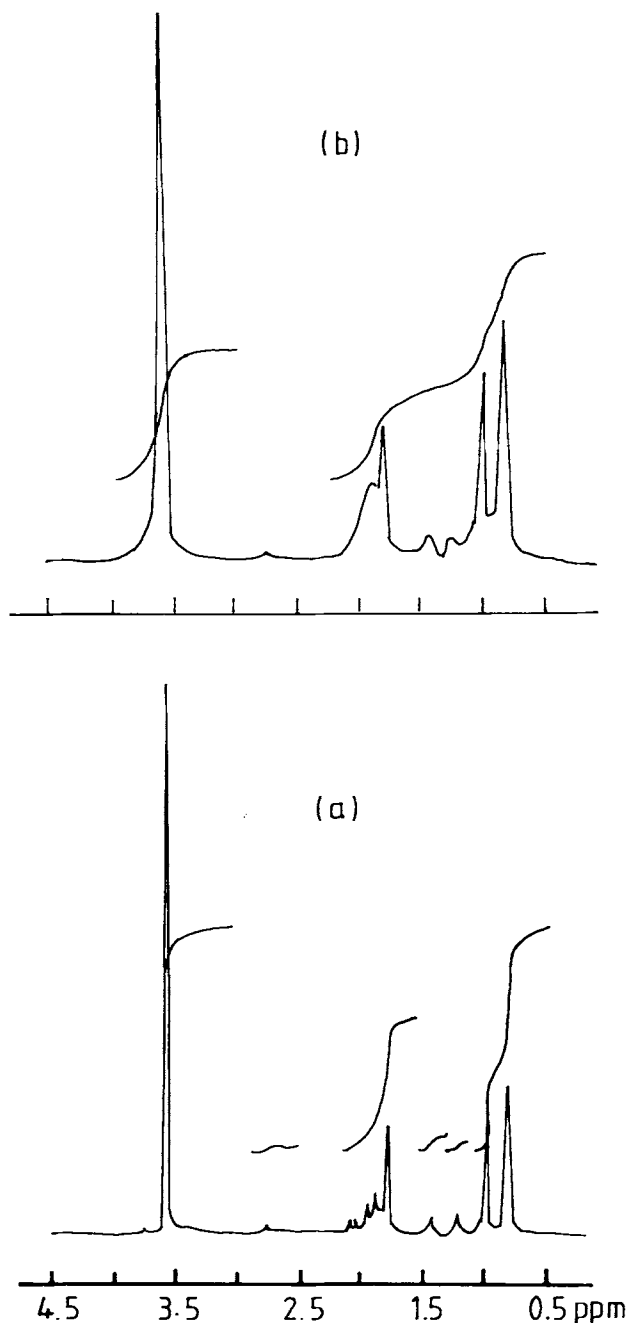


Figure 4 $^1\text{H-NMR}$ spectrum of (a) PMMA-ME and (b) PMMA-E.

emulsion medium showed \bar{M}_w 9.76×10^5 , \bar{M}_n 1.30×10^5 , and polydispersity 7.47. The polydispersity for both the polymers was observed to be higher, though for the microemulsion-based polymer it is comparatively lower. Similar results were observed by Gan and colleagues⁴ and Feng and Ng.³ The high polydispersity of both polymers may be due to the possibility of two types of nucleation: (1) nucleation in monomer droplets/monomer-swollen micelles,

and (2) homogeneous nucleation. Comparatively lower polydispersity for microemulsion-based polymer indicates predominance of nucleation in monomer droplets in microemulsion polymerization.

NMR Studies

Table II and Figure 4 show the signals obtained in high resolution $^1\text{H-NMR}$ of PMMA synthesized in microemulsion and emulsion media. The NMR signals for ester methyl resonance appear around 3.5 ppm, β -methylene protons appear around 2.0 ppm, and α -methyl protons appear between 1.5 and 1.0 ppm. The methylene resonance for the syndiotactic polymer is expected to give singlets as both the methylene protons will have similar environments in their immediate vicinity. However, an observed singlet shows broadening due to residual isotactic resonances, which complicates the spectrum with fine structures. We have observed two peaks at 1.89 and 1.80 ppm with broadening for PMMA synthesized in emulsion medium. The methylene resonance for the isotactic polymer is predominantly expected to give an AB quartet ($J = 14.9$ Hz) with additional syndiotactic resonance. This is because each of the two β -methylene protons are flanked either by both α -methyl protons or by ester methyl protons, creating a dissimilar environment in the immediate vicinity. For the PMMA synthesized from microemulsion medium we have observed five peaks between 2.06 and 1.81 ppm. J values for the second and third, and fifth and sixth peaks (Table II) were observed around 14 Hz and 13 Hz, respectively, indicating the dominant isotacticity in PMMA synthesized from microemulsion medium whereas syndiotacticity in PMMA synthesized from the emulsion medium.

These observations can be explained by the fact that in o/w microemulsion the monomer is present in microdroplets. During polymerization the monomer, in the microassemblies, is oriented with its hydrophilic part ($-\text{COOCH}_3$) toward the surface of the droplet. However, in the emulsion polymerization, propagation of the polymer chain takes place by diffusion of monomer from the monomer droplet reservoir, resulting in the products without specific orientation exhibiting products with predominant syndiotacticity.

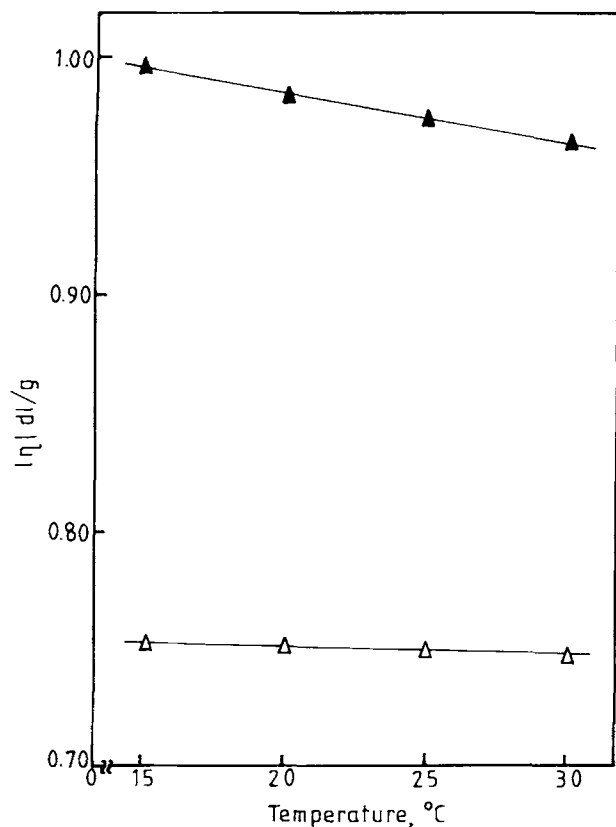
Thermal Studies

TGA of the PMMA synthesized in emulsion and microemulsion gave single-stage weight loss TG curves with degradation temperatures of 290°C to

Table III Intrinsic Viscosity, Viscosity Average Molecular Weights, and Hydrodynamic Volumes of PMMA Synthesized in Microemulsion (PMMA-ME) and Emulsion Media (PMMA-E)

	PMMA-ME				PMMA-E			
	15°C	20°C	25°C	30°C	15°C	20°C	25°C	30°C
$ \eta $ (dL/g) in acetone	0.753	0.752	0.751	0.750	0.995	0.985	0.975	0.965
$M_v \times 10^{-5}$			5.0				7.2	
V_e (mL/g) in acetone	28.45	28.32	28.10	27.95	37.70	37.50	37.27	37.05

420°C. From TG curves, activation energy was calculated using Briodo's equation.¹⁶ For the PMMA synthesized in microemulsion medium, activation energy was calculated to be 44.70 kJ/mol and that in emulsion medium 65.47 kJ/mol. This also indicates the difference in internal structure of PMMA synthesized through the above-mentioned routes. As less energy is required for degradation of PMMA synthesized in microemulsion medium, the product is expected to have relatively higher isotactic structure in comparison with PMMA synthesized in emulsion medium. This observation supports the results obtained in NMR study.

**Figure 5** Effect of temperature on intrinsic viscosity of (Δ) PMMA-ME and (\blacktriangle) PMMA-E.

Viscosity Studies

The effect of temperature on the hydrodynamic behavior of dilute polymer solutions can be studied through temperature dependence of the intrinsic viscosities (Table III and Fig. 5). It is observed that the intrinsic viscosity decreases in general with increase in temperature, though the effect is more pronounced in PMMA synthesized in emulsion medium. $|\eta|$ versus T plots are always linear with the negative slope, indicating that the polymer coils are not swelling to a great extent and lower critical solution temperature is exhibited by the PMMA synthesized through emulsion polymerization. This is due to decreased thermodynamic affinity with increased temperature.

The well known Frenkel-Eyring equation for viscous flow can be written as

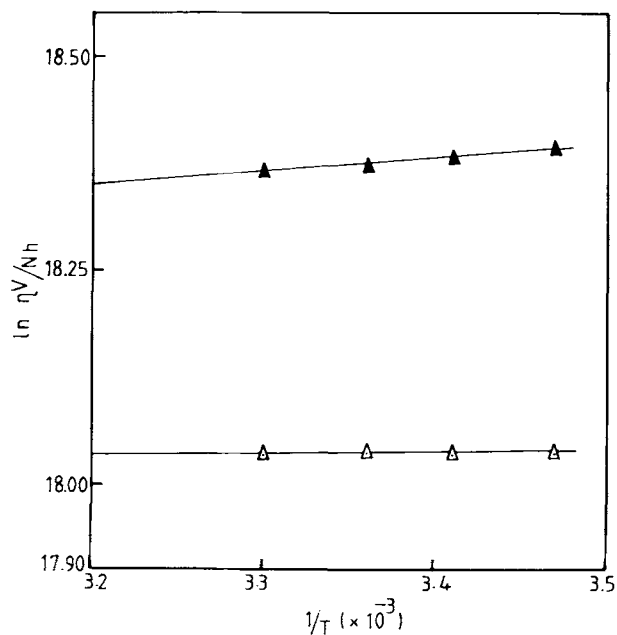
**Figure 6** Plots of $\ln(\eta V/Nh)$ versus $1/T$ for 0.5 g/dL solutions in acetone.

Table IV Intramolecular Expansion Factor and θ Solvent Compositions

Sample	θ Solvent Composition		$ \eta $	$ \eta _{\theta}$	α
	Acetone (%)	Methanol (%)			
PMMA-ME	56.90	43.10	0.751	0.587	1.085
PMMA-E	53.70	46.30	0.975	0.575	1.192

$$\eta = (Nh/V)\exp(\Delta G_{\text{vis}}^{\#}/RT) \quad (1)$$

where V is the molar volume and other symbols have their usual meanings. This equation can be rewritten as

$$\ln(\eta V/Nh) = (\Delta H_{\text{vis}}^{\#}/RT) - (\Delta S_{\text{vis}}^{\#}/R) \quad (2)$$

where $\Delta H_{\text{vis}}^{\#}$ and $\Delta S_{\text{vis}}^{\#}$ are enthalpy and entropy, respectively, for the viscous flow. Representative plots of $\ln(\eta V/Nh)$ versus T^{-1} are given in Figure 6 for PMMA synthesized in emulsion and microemulsion media, and show a linear relationship. The calculated values of $\Delta S_{\text{vis}}^{\#}$ and $\Delta H_{\text{vis}}^{\#}$ are 0.152 kJ/°C and 1.24 kJ/°C, respectively, for PMMA from emulsion system; and 0.150 kJ/°C and 0.16 kJ/°C, respectively, for PMMA from microemulsion system. The smaller values indicate no crosslinking in the PMMA.

The intramolecular expansion factor for the PMMA in solution was calculated from the intrinsic viscosity measurements in θ solvent at 25°C using an $\alpha^3 = |\eta|/|\eta|_{\theta}$ relationship. The spatial arrangement in the actual molecule is assumed to be expanded uniformly by the factor α as a result of intramolecular interaction. Table IV shows the θ solvent composition and intramolecular expansion factor. Though viscosity average molecular weight (\bar{M}_v) is smaller for PMMA from microemulsion system, θ solvent composition requires more solvent than that for PMMA from emulsion system. This may be because of the rigid structure of PMMA synthesized in microemulsion medium, whereas in the case of PMMA synthesized in emulsion medium the polymer chain is of relatively free nature. The smaller intramolecular expansion factor also indicates a more rigid (isotactic) structure for polymer synthesized in microemulsion medium. This also supports our NMR and TGA results. The relative viscosity data were used to calculate the equivalent hydrodynamic volume (voluminosity V_e), a measure of size of a solvated polymer molecule at infinite dilution. It was recently used to determine the shape

of protein molecules (natural polymers)¹⁷ and some acrylic polymers^{18,19} in solution. In the present study the same procedure was followed for the determination of V_e by plotting

$$Y = [(\eta_r^{0.5} - 1)]/[C(1.35 \eta_r^{0.5} - 0.1)]$$

versus C and extrapolating $C = 0$ to get V_e . The voluminosity is a function of temperature and is a measure of the volume of solvated polymer molecules. Hence, in the case of polymers which have more restricted structure, the volume of solvent required to solvate the polymer molecule is less in comparison with polymers which are less rigid in character. The lower molecular weight of the polymer may also result in lower hydrodynamic volume. Table III shows the hydrodynamic volume of polymers in acetone, which is less for PMMA synthesized in microemulsion medium than in emulsion medium. As the temperature increases the solvation decreases; hence V_e decreases. From $|\eta| = \nu V_e$, the shape factor ν was calculated. It was observed that value of ν for all systems at all temperatures remains constant at 2.6. This indicates that in the concentration range studied, the polymer molecules are spherical.

CONCLUSION

Microemulsion polymerization of MMA follows a two-stage process whereas emulsion polymerization follows a three-stage process. Due to the relatively high solubility of monomer, homogeneous polymerization is expected to be important in both emulsion and microemulsion polymerization. However, in the microemulsion the nucleation is observed to be mainly in the microemulsion droplets. The difference in polymerization mechanism resulted in products with different internal structures, which was confirmed through NMR, thermal, and viscometric studies.

We are thankful to Asian Paints (India) Ltd. for financial support for this work. We are grateful to Prof. Girjesh Govil, Tata Institute of Fundamental Research, Bombay, for the high-resolution $^1\text{H-NMR}$ analysis.

REFERENCES

1. J. O. Stoffer and T. Bone, *J. Disp. Sci. Technol.*, **1**, 37 (1980).
2. J. Jaykrishnan and D. O. Shah, *J. Polym. Sci., Polym. Lett. Ed.*, **22**, 31 (1984).
3. L. Feng and K. Y. S. Ng, *Macromolecules*, **23**, 1048 (1990).
4. L. M. Gan, C. H. Chew, S. C. Ng, and S. E. Loh, *Langmuir*, **9**, 2799 (1993).
5. W. D. Harkins, *J. Am. Chem. Soc.*, **69**, 1428 (1947).
6. W. V. Smith and R. H. Ewart, *J. Chem. Phys.*, **16**, 592 (1948).
7. B. Jacobi, *Angew Chem.*, **64**, 539 (1952).
8. R. M. Fitch, *British Polym. J.*, **5**, 467 (1973).
9. R. Patsiga, M. Litt, and V. Stannet, *J. Phys. Chem.*, **64**, 801 (1960).
10. H. I. Tang, P. L. Johnson, and E. Gulari, *Polymer*, **25**, 1357 (1984).
11. J. S. Guo, M. S. El-Aasser, and J. W. Vanderhoff, *J. Polym. Sci., Polym. Chem. Ed.*, **27**, 691 (1989).
12. P. L. Kuo, N. J. Turro, C. M. Tseng, M. S. El-Aasser, and J. W. Vanderhoff, *Macromolecules*, **20**, 1216 (1987).
13. V. H. Perez Luna, J. E. Puig, V. M. Castano, B. E. Rodriguez, A. K. Murthy, and E. Kaler, *Langmuir*, **6**, 1040 (1990).
14. J. H. Baxendale, S. Byewater, and M. G. Evans, *Trans. Faraday Soc.*, **42**, 675 (1946).
15. W. S. Zimmt, *J. Appl. Polym. Sci.*, **1**, 323 (1959).
16. A. Broido, *J. Polym. Sci., Part A-2*, **7**, 1761 (1969).
17. A. S. Narang and V. L. Garg, *J. Indian Chem. Soc.*, **66**, 214 (1989).
18. R. Joseph, S. Devi, and A. K. Rakshit, *Polym. Int.*, **26**, 89 (1991).
19. A. K. M. Asaduzzaman, A. K. Rakshit, and S. Devi, *J. Appl. Polym. Sci.*, **47**, 1813 (1993).

Received November 30, 1995

Accepted April 8, 1996